Comparative X-Ray Diffraction Study of SnO$_2$ Nanoparticle Samples from Different Precursor Solutions

S. P. Choudhury[1], N. Kumari[2], A. Bhattacharjee[1, 3]

[1]National Institute of Technology Meghalaya, Shillong, Meghalaya-793003

[2]Indian Institute of Technology Delhi, New Delhi-110016

[3]National Institute of Technology Silchar, Silchar, Assam-788010

Abstract: *SnO$_2$ is n-type semiconductor and a transparent conducting oxide, and has apt properties in a gas sensing material, photovoltaic cells, fuel cells, batteries etc. In the present work SnO2 nanoparticles were synthesized by two different methods using different precursors. In method 1 using SnCl$_4$.5H$_2$O a particle size of about 37nm was obtained and in method 2 using SnCl$_2$.2H$_2$O precursor, the size of the obtained nanoparticles were of the order of 9nm. XRD studies were conducted on the samples obtained by method 1 and method 2 to ascertain the composition and particulate size. Using the Williamson Hall plot some important properties like lattice strain, lattice parameters and effective particle size was calculated. The work revealed the solvent effect as well as pH dependency for controlling the particle size. The addition of capping agent (HCl) was decisive in lowering the particle size and setting up a possible quantum confinement study base on sample 2 with better understanding of the reaction mechanism.*

Keywords: SnO2, TCO, Williamson Hall Plot, nanoparticles

1. Introduction

Broad band doped n-type semiconductors are considered preferable for real life applications. One of the most successful n-type metal oxide semiconductor is SnO$_2$ which has found wide applications in gas sensors. The variation in the electrical resistance of the semiconductor oxide films when the gas of interest interacts with its surface is what motivates the scientific society for its application in gas sensors [1]. Our aim was to synthesize a SnO2 samples of different grain size and characterize them.

The variation of electrical conductivity from ~10^{-6} S/cm [2] to 0.4-1.2 x 10^4 S/cm [3, 4] was attainable for SnO$_2$ under different conditions. This variation can be attributed to the structure of SnO$_2$ with a suitable band gap. This very property scores over other semi-conductor metal oxides.

As already mentioned the wide band gap of 3.6 ev at a temperature of 300°C was one of the decisive factors for influencing electrical and optical properties of SnO$_2$ [5]. Considering one of the major application of SnO$_2$ in gas sensors semiconductor oxides like SnO$_2$ [6], TiO$_2$, Fe$_2$O$_3$, WO$_3$, InO$_3$, MoO$_3$ have been studied to detect gases like H$_2$, CH$_4$, CO, CO$_2$, NO$_x$, H$_2$S and O$_2$. Considering the grain boundary as a potential barrier which has an influence on the resistance, the particle size plays a vital role for the sensitivity at a lower temperature [2, 7]. Hence the procedure needed to be followed for the synthesis of SnO$_2$ or any other semiconductor metal oxides should generate particle size in the nanometer range preferably within 10nm [1, 8]. But as the particle size increases the sensitivity keeps on decreasing. The same can be consolidated with the addition of dopants like palladium, platinum, silver [9, 10] and also by some basic oxides [10, 11]. This property was attributed to the increase in the space charge width [10]. However the addition of impurity should have some characteristics as for example it should be trivalent, noble metal or their oxides and should have a valency of less than +4 in the oxide lattice.

Different applicable procedures for the preparation of SnO$_2$ nanoparticles have been confirmed in different papers. Some of the prominent methods involve that by co-precipitation [12], Sol-gel [13], spray pyrolysis [14] and hydrothermal routes [15]. Our study involves the preparation of two different samples of SnO$_2$ nanoparticles by chemical co-precipitation method by using two different precursors SnCl$_2$.2H$_2$O and SnCl$_4$.5H$_2$O. We were able to identify a better sample for fabrication of SnO$_2$ gas sensor which lies in our future plan of work.

2. Experimental

2.1 Synthesis

Synthesis of SnO$_2$ was carried out by two different chemical routes. In method 1 SnO$_2$ nanoparticles were prepared by using SnCl$_4$.5H$_2$O as precursor. Distilled water was added to a particular amount of SnCl$_4$.5H$_2$O to obtain a molar concentration of 0.1 M. Thereafter 4 ml of ammonia was added and stirred for 20 minutes. A white gel like precipitate evolved which was allowed to settle down for 12 hours. The solution was continuously washed with distilled water to remove the chloride content. The obtained sample was then heated for approximately 24 hours at a temperature of 70°C for removing the water content and a fine power was obtained. In method 2 1 gm of the precursor, stannous chloride dihydrate (SnCl$_2$.2H$_2$O) was added to a solution of 11 ml deionized water and 5 ml of Ethanol and was continuously stirred for 10 minutes using magnetic stirrer. Thereafter 1 ml of HCl was added drop wise and the solution was stirred for another 20 minutes. Aqueous ammonia was

added drop wise to the obtained clear solution. With the help of a digital Mettler Toledo pH meter the pH of the solution was kept constant at 8.5. A milky white solution was obtained which was continuously stirred in the magnetic stirrer for 2 hours. The particles were then allowed to settle down for 15 hours. Thereafter it was washed with distilled water and ethanol to remove the chloride content. Finally the sample was heated at a temperature of 80°C to remove the remaining water content and the sample was obtained in the powder form.

For the calculation of the porosity, the samples prepared by method 1 and method 2 were pelletized by dye and punch method under a pressure of 5 Mp and pellets of diameter 13mm and thickness 2 mm were formed.

2.2 Characterization

The structural characterization of the samples were carried out by Panalytical X'pert Pro X-ray diffractometer with Cu-Kα (λ=0.15418 nm) as X-ray source at 40 kV and 30 mA with scanning angle (2θ) ranging from 20° to 90°. The obtained spectra were analyzed using the X-pert Highscore Software.

3. Results and discussions

Figure 1 shows the XRD spectra of the samples prepared by method 1 and method 2. The data were corrected for background, Kα₂ stripped, fitted and refined.
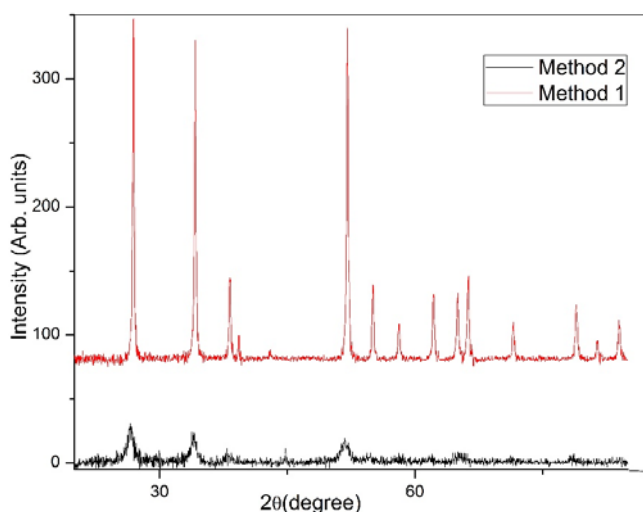
Figure 1: XRD Spectra of SnO2 samples prepared by method 1 and method 2

The XRD analysis confirms the sample as SnO_2. The obtained peaks were comparable to the SnO_2 JPCDS card no: 41-1445 data. The XRD pattern in figure 1 shows the characteristic tin oxide peaks. The non-existence of any other overlapping peak in the standard peak positions indicates that the prepared sample has a single phase, i.e. the existence of only SnO_2 molecules. Various parameters determined by XRD are tabulated in table 1.

Table 1: 2θ, FWHM, d-spacing, relative intensity and crystallite size (FWHM is the full width at half of the peak maximum, θ is the Bragg's angle, d-spacing represents the interplanar distance and (hkl) refers to the miller indices)

Properties	Planes (hkl)	Method 1	Method 2
2θ (degrees)	110	26.917	26.5678
	101	34.1874	33.9825
	211	52.0782	51.7738
FWHM (degrees)	110	0.2141	0.817
	101	0.229	0.8802
	211	0.2347	1.1809
d-spacing (Å)	110	3.30968	3.35239
	101	2.62065	2.63598
	211	1.75473	1.76433
Relative intensity	110	332.42	38.05
	101	302.32	27.07
	211	267.29	23.63
Crystallite Size (nm)	110	37.7391	9.8826
	101	35.9006	9.3351
	211	37.2637	7.3965

The crystallite size was calculated by employing well known Scherrer formula as in equation (1) [17]:

$$D = \frac{k\lambda}{\beta\cos\theta} \qquad (1)$$

where D stands for the mean crystallite size, K is a particle size dependent constant whose value is 0.9, β represents the full width at half of the peak maximum (FWHM) and θ is the Bragg's angle. The crystallite size was calculated to be approximately 37nm and 9nm for method 1 and 2 respectively.

The standard values of the lattice parameters for SnO_2 was a = 4.737 Å and c = 3.185 Å. The values calculated for lattice parameter a and c and lattice distortion u are tabulated in table 2.

Table 2: Lattice parameters, lattice distortion and cell volume

Properties	Method 1	Method 2
a (Å)	4.687	4.741
c (Å)	3.161	3.171
U	1.483	1.495
Cell Volume	69.446	71.281

The lattice parameters for the tetragonal phase structure was calculated using relation (2) [14]:

$$\frac{1}{d^2} = \left(\frac{h^2 + k^2}{a^2}\right) + \frac{l^2}{c^2} \qquad (2)$$

The lattice distortion was given by relation 3 [16]:

$$U = \frac{a}{c} \qquad (3)$$

The values being comparable to the standard value assures the fact that the prepared sample was SnO_2 and it has a rutile structure. The strain dependent change of properties when the sample was prepared by the two methods was highlighted by the changed lattice parameters values. The value of both the lattice parameters decreases in method 1 in comparison to method 2 resulting in a decrease in the lattice distortion and cell volume.

The porosity of the two samples were calculated. The porosity being given as a ratio of the pore volume and the bulk volume was calculated by employing relations (4)-(6):

Paper ID: ETPTA-119

45

International Journal of Science and Research (IJSR), ISSN (Online): 2319-7064, Impact Factor (2012): 3.358, www.ijsr.net

$$\rho_x = \frac{nM}{Na^2c} \qquad (4)$$

$$\rho_a = \frac{m}{v} = \frac{m}{\Pi r^2 h} \qquad (5)$$

$$P = \left(1 - \frac{\rho_a}{\rho_x}\right) X 100\% \qquad (6)$$

where ρ_x denotes the total volume, ρ_a denotes the volume of solid, n is the number of molecules per unit cell, M is the molecular weight, a and c denotes the lattice parameters, N is the Avogadro's number, m, v, r and h denotes the mass, volume, radius and thickness of the pellets.

The porosities were calculated to be 74.4117 and 78.1797 respectively for samples prepared by method 1 and method 2 respectively. Though the change in porosity was small it still indicates that the preparation of the sample by method 2 where particle size are smaller will give better results in sensing materials. This is because of the fact that a smaller particle size gives higher surface to volume ratio allowing the gas to penetrate a deeper depth which in turn results in better response and higher gas sensitivity [18, 19].

The Williamson Hall plot for both the samples was plotted between $\beta\cos\theta/\lambda$ and $\sin\theta/\lambda$ as in figure 2.
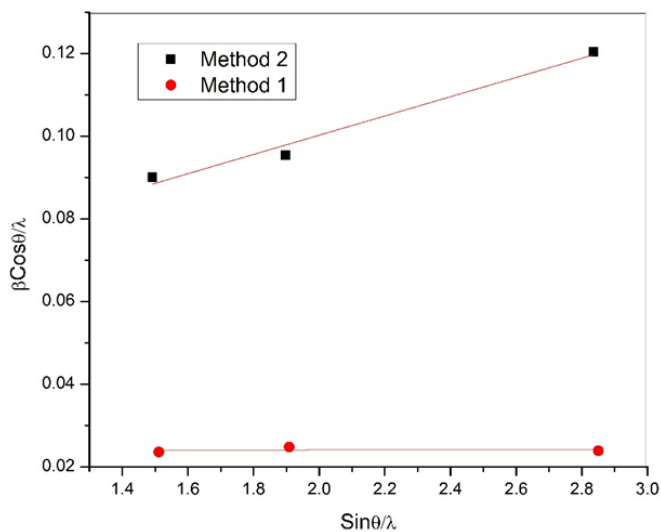
Figure 2: WH plot of SnO$_2$ samples prepared by method 1 and method 2

The existence of tensile or compressive strain can be determined from the WH Plot by finding the slope of the curve and employing the relation (7) [20]

$$\frac{\beta\cos\theta}{\lambda} = \frac{1}{D} + \frac{\varepsilon\sin\theta}{\lambda} \qquad (7)$$

where β was the FWHM of the concerned peak and D was the average grain size. The application of the Williamson and Hall equation determines the lattice parameters, strain and the effective particle size.

The lattice parameters and the crystallite size were interdependent. From table 1 and table 2 it was seen that for method 1 the crystallite size was more and cell volume less as compared to method 2. The percentage decrease in the

cell volume was 2.58. This decrease of the cell volume indicates the existence of more tensile strain in case of method 2 in comparison to method 1. With the decrease of the particle size in method 2 the lattice distortion increases from 1.483 to 1.495 further confirms the tensile state of the lattice in method 2.

From Table 1 the increase of d-spacing in method 2 in the different planes indicates tensile strain in method 2. Hence XRD further confirms the result calculated by WH Plot. An increase in the FWHM value results in the decrease of the particle size in case of method 2 as calculated by the Debye-Scherrer formula. The smaller the particle size more would be the surface to volume ratio resulting in more adsorption. This would affect the sensing effectively. Further the increase of FWHM values as we move from plane (110) to (211) for method 1 and method 2 individually can be attributed to the presence of non-uniform strain which changes from one plane to another plane. The calculation of the effective particle size from the WH Plot shows the particle size in method 2 was 18.6 nm while that in case of method 1 was 41.5 nm. This particle size was determined from intercepts of the curve. The variation in the value of the particle size calculated by Debye Scherrer formula and by WH Plot can be attributed to the fact that WH Plot takes the lattice strain into consideration.

As observed in the WH plot the slope was positive indicating the existence of tensile strain in both cases. The strain in case of method 1 was 0.101 x 10^{-4} while that in case of method 2 was 0.233 x 10^{-1}. A higher value of the slope in case of method 2 suggests more tensile strain in this case with the decrease in the particle size.

4. Conclusion

Two different methods were employed for SnO2 nanoparticles preparation and by XRD analysis it was revealed that the nanoparticles formed was indeed SnO2 and sizes were 37nm and 9nm for the two different methods. The porosities were calculated to be 74.4117 and 78.1797 for the two samples. The data also points out that the existence of tensile strain was more in the second case. The WH plot was instrumental in determining the lattice parameters, strain and effective particle size. The second method lowered the particle size considerably. The quantum confinement effect comes into play below a size of 10nm. The particle size should be comparable to Bohr radius and should be near about 2-3nm. So with further refinement and change in the synthesis process we intend to reduce the size further in our future work.

References

[1] M.J. Madou, S.R. Morrison, Chemical sensing with solid state devices, Academic Press, San Diego, 1999
[2] S.K. Song, J.S. Cho, W.K. Choi, H.J. Jung, D. Choi, J.Y. Lee, H.K. Baik, S.K. Koh, "Structure and gas-sensing characteristics of undoped tin oxide thin films fabricated by ion-assisted deposition", 46, pp. 42, Sens. Actuators, 1998.

[3] C. Agashe, B.R. Marathe, M. G. Takwale, V.G. Bhide, "Structural properties of SnO2: F films deposited by spray pyrolysis technique", 164, pp. 261, Thin Solid Films, 1988.

[4] H.S. Randhawa, M.D. Matthews, R.F. Bunshah, "SnO2 films prepared by activated reactive evaporation", 83, pp. 267, Thin Solid Films 1981.

[5] X.H. Vu,T.H.A. Ly, Q.T. Khuc, D.V. Dang, D.C. Nguyen, "LPG sensing properties of SnO2 nanoparticles doped with several metal oxides by a hydrothermal method", 1, pp.025014, Adv. Nat. Sci. Nanosci. Nanotechnol., 2010.

[6] E.R. Leite, I.T. Weber, E. Longo, J.A. Varela, "A new method to control particle size and particle size distribution of SnO2 nanoparticles for gas sensor applications", 12, pp. 965-968, Adv. Mater., 2000.

[7] C. Xu, Tech. Digest, 9th Sensor Symp., International Academic Publishers, Beijing, pp. 95-98, 1990.

[8] F. Lu, Y. Liu, M. Dong, X.P. Wang, "Nanosized tin oxide as the novel material with simultaneous detection towards CO, H_2 and CH_4", 66, pp. 225-227, Sens. Actuators B, 2000.

[9] N. Yamazoe, Y. Kurokawa, T. Seiyama, "Effects of additives on semiconductor gas sensors", 4, pp. 283-289, Sensors and Actuators 1983.

[10] N. Yamazoe, "New approaches for improving semiconductor gas sensors", 5, pp. 7-19, Sensors and Actuators B, 1991.

[11] G. Heiland, "Homogenous semiconducting gas sensors", 2, pp. 343-361, Sensors and Actuators B 1982.

[12] A.C. Bose, P. Balaya, P. Thangadurai, S. Ramasamy, "Grain size effect on the universality of AC conductivity in SnO2", 64, pp. 659-663, J. Phys. Chem. Solids, 2003.

[13] O.K. Varghese, L.K. Malhotra, G.L. Sharma, "High ethanol sensitivity in sol–gel derived SnO2 thin films", 55, pp. 161-165, Sens. Actuators B 1999.

[14] R.R. Kasar, N.G. Deshpande, Y.G. Gudage, J.C. Vyas, R. Sharma, "Studies and correlation among the structural, optical and electrical parameters of spray-deposited tin oxide (SnO_2) thin films with different substrate", 403, pp. 3724-3729, Physica B 2008.

[15] H.C. Chiu, C.S. Yeh, "Hydrothermal synthesis of SnO2 nanoparticles and their gas-sensing of alcohol", 111, pp. 7256-7259, J. Phys. Chem. C 2007**.

[16] N.S. Ramgir, Y.K. Hwang, I.S. Mulla, J.S. Chang, "Effect of particle size and strain in nanocrystalline SnO_2 according to doping concentration of ruthenium", 8, pp. 359-362, Solid State Sciences 2006.

[17] S. Chacko, N.S. Philip, K.G. Gophandran, P. Koshy, V.K. Vaidyan, "Nanostructural and surface morphological evolution of chemically sprayed SnO_2 thin films", 254, 2179-2186, Appl. Surf. Sci. 2008.

[18] M.H. Seo, M. Yuasa, T. Kida, J. SooHuh, K. Shimanoe, N. Yamazoe, "Gas sensing characteristics and porosity control of nanostructured films composed of TiO_2 nanotubes", 137, pp. 513-520, Sensors and Actuators B, 2009.

[19] M.S. Wagh, L.A. Patil, T. Seth, D.P. Amalnerkar, "Surface cupricated SnO_2–ZnO thick films as a H_2S gas sensor", 84, pp. 228-233, Materials Chemistry and Physics 2004.

[20] M. Dhanam, P.K. Manoj, R. Rajeev, R. Prabhu, "High-temperature conductivity in chemical bath deposited copper selenide thin films", 280(3-4), pp. 425-435, J. Crystal Growth 2005.

Author Profile

Sandip Paul Choudhury received the Masters degree in Physics from North Eastern Hill University, Shillong, India. Thereafter he completed a DST project as a JRF in Visva-Bharati University, Shantiniketan, India. He is currently pursuing his PhD from NIT Meghalaya, Shillong.